Iranian Journal of Hydrogen & Fuel Cell 2(2017) 139-151

Iranian Journal of Hydrogen & Fuel Cell

IJHFC

Journal homepage://ijhfc.irost.ir

The effect of solvent of titanium precursor in the sol-gel process on the activity of TiO_2 nanoparticles for H_2 production

M.Taherinia, M.Nasiri*, E.Abedini, H. R. Pouretedal

Department of Chemistry, Malek-ashtar University of Technology, Shahin-Shahr, Isfahan, Iran

Article Information

Article History:

Received:
31 July 2017
Received in revised form:
24 Oct 2017
Accepted:
04 Nov 2017

Keywords

H_2 production
Solar light
TiO_2 nanoparticles
Photocatalyst

Abstract

A modified sol-gel process has been found to significantly improve the photocatalytic activity of TiO_2 nanoparticle in the process of solar hydrogen production. The surface of TiO_2 nanoparticles were modified by the optimization of solvent of titanium precursor (acetic acid and/or ethanol) in the sol-gel method. A multi technique approach (SEM, XRD, FTIR, UV-DRS and TGA) was used to characterize the prepared TiO_2 nanoparticles. The photocatalytic hydrogen production was tested using a suspension of photocatalyst TiO_2 at 10 vol. % methanol under natural solar light. The produced hydrogen was subjected to gas chromatography with a continuous flow of N_2 in the photoreactor system. It was found that the TiO_2 nanoparticles synthesized with acetic acid as the solvent of titanium precursor, TiO_2-AA, have a better photocatalytic activity for hydrogen production compared to nanoparticles synthesized with ethanol, TiO_2-EA. The obtained results showed that the better crystallinity, small size and proper surface properties of TiO_2-AA nanoparticles is due to higher photoactivity.

1. Introduction

Hydrogen has high energy efficiency without any environmental pollution [1, 2]. Nowadays, hydrogen is obtained from steam reformation of natural gas, liquefied hydrocarbons, and liquefied petroleum gas [3, 4]. Although, industrial production of hydrogen consumes high level of energy and produces huge

*Corresponding Author's Fax: +983145220420
E-mail address: nasiri@mut-es.ac.ir

doi:10.22104/ijhfc.2017.2372.1147

amount of carbon dioxide as by-product and greenhouse gases [1]. The photocatalytic splitting of water under sunlight for producing hydrogen is one of the potential methods for getting clean, low cost and eco-friendly fuel [4]. Titanium dioxide as a photocatalyst has been the subject of interest for many researchers because of its several advantages such as non-toxicity, eco-friendly feature, availability and chemical stability. Titanium dioxide exists in nature in three phases; rutile, anatase and brookite [3, 5]. Photocatalytic activity of titanium dioxide depends on its crystal structure, degree of crystallinity and specific surface. The anatase phase has more photocatalytic activity than the other two phases due to its greater crystallinity and surface, and smaller particle size [6, 7]. There are several methods for synthesizing nanoparticles such as sol-gel, hydrothermal, precipitation and flame synthesis. The morphology, structure and photocatalytic activity are dependent on the method of synthesizing nanoparticles [8–10]. Because of a wide range of advantages, the sol-gel method has attracted the focus of many researchers. Some of the notable advantages includes high chemical purity, high homogeneity, fine-scale and controllable morphology [6, 11]. In this method, the precursor molecule (usually metal alkoxides) is hydrolyzed in a solvent and a colloidal dispersion of sol is formed. The accumulation of sol particles creates an infinite network of particles which consequently leads to the gel production. The resulting gel is dried and then powdered and the obtained powder is heated for calcination [6]. Alkoxides precursors, such as titanium butoxide and titanium isopropoxide, are usually used to produce titanium dioxide nanoparticles, and the precursor is generally dissolved in an alcoholic solvent (for instance ethanol) [12, 13]. Making changes in the synthesis method to obtain TiO_2 nanoparticles with more suitable properties have been reported in multiple research. In 2014 Xin and coworkers synthesized TiO_2 nanoparticles using the hydrothermal method and examined the effect of calcination temperature on the material's properties and its photocatalytic activities in producing Hydrogen [15]. R. Vijayalakshmi and V. Rajendran compared two methods, hydrothermal and sol-gel, for synthesizing TiO_2 nanoparticles in the same ambient conditions, they reported that the synthesized particles using the sol-gel method have more crystallinity and smaller size than the particles synthesized using the hydrothermal method [16]. Loryuenyong and coworkers synthesized TiO_2 nanoparticles using the sol-gel method with isopropanol as solvent and active carbon as templates, they reported an increase in the specific surface of the synthesized TiO_2 nanoparticles and an increase in the band gap (0.3 to 0.6 eV) that could be due to the effect of restricted movement of electrons [17]. Lou and coworkers also synthesized TiO_2 using the sol gel method with the help of polyethylene glycol (PEG) and cetytrimethy lammonium bromide (CTAB) and examined the effect of their presence on the size of the particles [18]. Dinh and coworkers have synthesizied TiO_2 using the solvothermal method using water as the agent of hydrolysis and oleic acid (OA) and oleylamine (OM) as two distinct capping surfactants, and by changing this factor they examined their effect on the crystallinity and the shape of the particles [19]. Sanaz Naghibi and coworkers used the Taguchi method have examined the different factors, such as pH and precursor of Ti, they used the sol-gel and then hydrothermal method for synthesizing nanoparticles with the highest crystallinity and smallest particle size .[20] One common method for synthesizing nanoparticles is the sol-gel method with the help of an organic solvent. In 2015, Zhang and partners synthesized TiO_2 nanoparticles using the sol- gel method with the use of DMAC as a solvent and glacial acetic acid as a catalyst and researched the effect of the ratio between the solvent and TBT amount [21]. In sol-gel processes, the morphology of the final product is strongly influenced by the reactivity of the precursor [14]. So it is an important subject to consider in the details of this method, since the details play an important role in the size of particles and photocatalytic activity of TiO_2 in processes such as water splitting.

In the present work, TiO_2 nanoparticles were synthesized via the sol-gel route with two different

solvent of Ti precursor, acidic solvent and alcoholic solvent. We present the effect of the solvent of titanium precursor on the characterizations of TiO_2 nanoparticles. The photocatalytic activity of TiO_2 was investigated by water splitting and the production of H_2 under natural solar light.

2. Experimental

2-1.Preparation of TiO_2 nanoparticles

All the chemical materials were purchased from Merck and were used without any further purification. The TiO_2 nanoparticles were synthesized by the sol-gel method in solvents of glacial acetic acid (AA) and/or anhydrous ethyl alcohol (EA) as a precursor solvent. The titanium tetraisopropoxide (TTIP) was used as the precursor of titanium. The prepared TiO_2 nanoparticles in solvents of glacial acetic acid (AA) and anhydrous ethyl alcohol (EA) were named as TiO_2-AA and TiO_2-EA, respectively.

In an experimental route, the titanium tetraisopropoxide as precursor (8 ml TTIP) was solved in 40 ml of absolute ethanol and /or acetic acid in room temperature. Forced hydrolysis of the TTIP solution was achieved by adding a certain volume of deionized water (40 ml). Subsequently, the solutions were ultrasonicated (Modle; Hielscher UP400S) for 15 min and then the stirring process was continued for a further 30 min, the solutions were again ultrasonicated for 15 min until a clear solution was formed. The prepared solutions were kept in an oven at 70 °C for 16 h. The gels of TiO_2-AA and TiO_2-EA were dried at 120 and 100 °C, respectively. The prepared powders were crushed well and calcinated in air in the muffle furnace for 2 h at different temperatures. The as-synthesized samples were denoted as TiO_2-AA-X and TiO_2-EA-X, where x refers to the calcination temperature.

2.2. Catalyst characterization

Thermal Gravimetric Analysis (TGA) was carried out for the titanium dioxide samples using simultaneous TGA, model of Perkin-Elmer, and STA-6000 under Ar atmosphere with a heating rate of 10 °C.min^{-1}. The XRD patterns were recorded on a Philips X'pert Pro MPD model using Cu Kα radiation as the X-ray source. The diffraction pattern was taken in the 2θ range 10–80°. The average crystallite size of the anatase phase was determined according to the Scherrer equation. The morphology and size of the nanoparticles were characterized using a scanning electron microscope (SEM, Philips XL-30ESM). Fourier transform infrared spectra (FT-IR) was measured by a JASCO 6300 spectrophotometer (200–4000 cm^{-1}). UV–Vis diffuse reflectance spectra (DRS) were determined by a UV–Vis Spectrophotometer (JASCO, V-670).

2.3. Photocatalytic hydrogen production

Photocatalytic hydrogen evolution experiments were carried out in a self-designed system under natural solar light as shown in Fig. 1. The reaction was typically performed in a pyrex reactor by adding 0.2 g catalyst to a solution of deionized water (270 ml) and methanol (30 ml) under stirred condition. The reactor was then sealed and before the irradiation, the mixture was degased with nitrogen gas for about 30 min to completely remove any oxygen. A nitrogen gas flow (100 mL/min) was passed through the mixture during the irradiation. A magnetic stirrer was used for uniform dispersion of the catalysts in the reactor during solar irradiation. The amount of H_2 produced was measured using online gas chromatography (Agilent 6890N) equipped with an injection valve (VALCO type), a molsieve 5A column, a TCD detector and N_2 as carrier gas. The calibration plot was obtained by using GC with high purity H_2 and N_2 gases and injected with different concentrations. The results of blank tests showed that the presence of photocatalyst, solar light and scavenger are essential for H_2 generation. For comparison, the H_2 evolution rate using the commercial photocatalyst Degussa P25 was also determined following the same procedure described

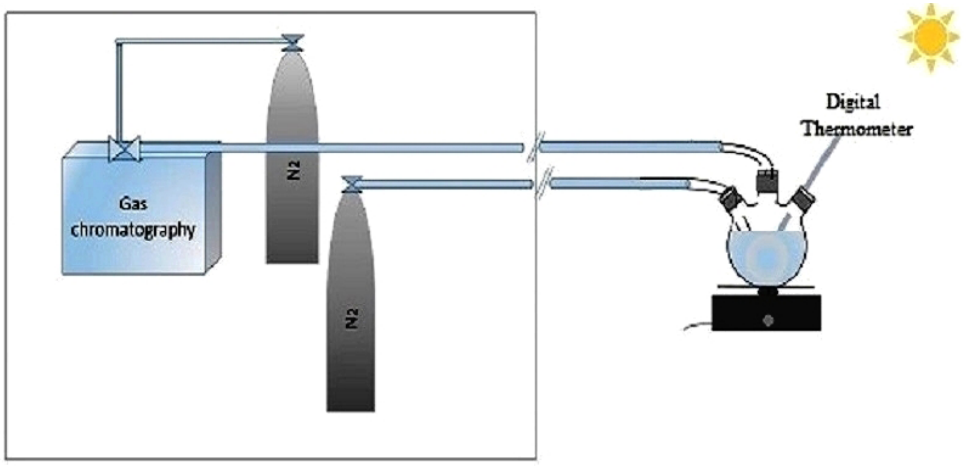

Fig. 1. Schematic representation of experimental setup for photocatalytic water splitting under solar irradiation.

above. The photocatalytic hydrogen production under solar light has been investigated at 12:00 am to 3:00 pm in the summer season in Esfahan, Iran (32°5'N, 51°43'E).

3. Results and discussion

3.1. Characterization of nano-TiO_2

TGA/DTGA profile of representative TiO_2-AA and TiO_2-EA samples are shown in Fig. 2. The total of mass loss is 21% for TiO_2-AA and 11% for TiO_2-EA. The TGA curve (Fig. 2 a) shows that the mass loss for TiO_2-AA occurs in two different stages. The first step of mass loss (5.4 %) is in the temperature range of 50 to 250 ºC, which is related to the dehydration and evaporation of organic substances [22, 23]. The second step of mass loss (13.9 %) is seen in the range of 250 to 410 ºC that is assigned to the burnout of hydroxyl groups and the organic substances [22, 24]. The TGA curve of TiO_2-EA is shown in Fig.2b. The TiO_2-EA does not have a separate decomposition temperature. Instead, it exhibits a gradual mass loss (11%) from 50 to 700 ºC. The TG curve of TiO_2-EA shows an initial mass loss of ~6% at nearly 50 °C and continuing until 200°C attributable to physisorbed water and ethanol solvents [25, 26]. In the range of 200 to 420 ºC, the second step of mass loss (3.6%) that is related to the removal of hydroxyl groups and other organic groups [24] is seen with a peak of DTGA at around 397 °C. The DTGA curve of TiO_2-AA clearly shows the two peaks with different heights at around 309.34 and 364.45 °C. These peaks are related to the decomposition of organic compounds which participate in the synthesis [22].

X-ray diffraction (XRD) is one of the oldest and most useful approaches in identifying crystalline materials [27]. XRD analysis was carried out in the range of 2θ=10–80 for samples to investigate the structural changes of TiO_2 affected by synthesis methods, as demonstrated in Fig. 3. The synthesized nanoparticles showed crystalline nature with the pure anatase phase of TiO_2. The diffraction peaks at 25.44◦, 37.95◦, 48.21◦, 54.034◦, 55.22◦, 62.82◦, 68.91◦, 70.46◦ and 75.23◦ correspond to the crystal planes [101], [004], [200], [105], [211], [204], [220], [220] and [215], respectively; this is attributed to reflections of anatase TiO_2 which is compared with JCPD Card No.(21-1272) [16, 28].

The average crystallite size of the synthesized TiO_2-AA and TiO_2-EA were calculated by using Scherrer's equation. According to Scherrer's formula, ($D = 0.9\,\lambda / (\beta \cos\theta)$ where D is the average crystallite size (nm), λ is the applied X- ray wavelength (λ =0.15406 nm), θ is the diffraction angle and β is the full width at half maximum (FWHM) [16]. The size of nanoparticles from the strongest peak (at 2θ of 250) was calculated [29]. According to this formula, the average crystallite sizes of TiO_2-AA-450 and TiO_2-EA-450

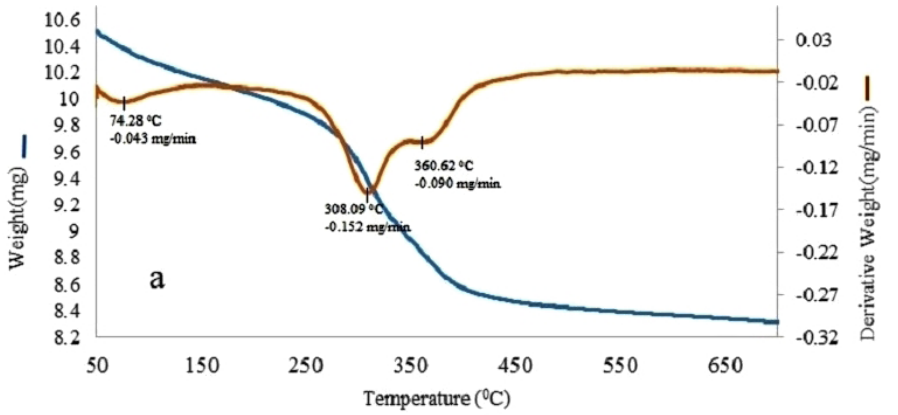

(a)

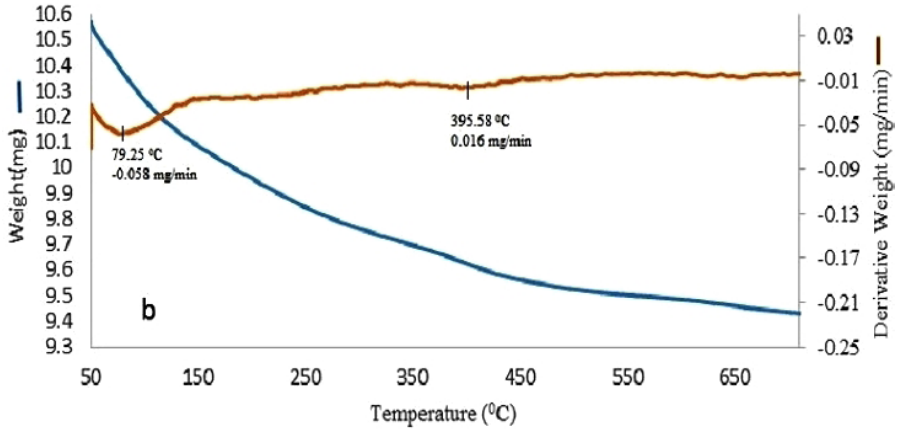

(b)

Fig. 2. TGA/DTGA curves of a) TiO_2-AA, b) TiO_2-EA.

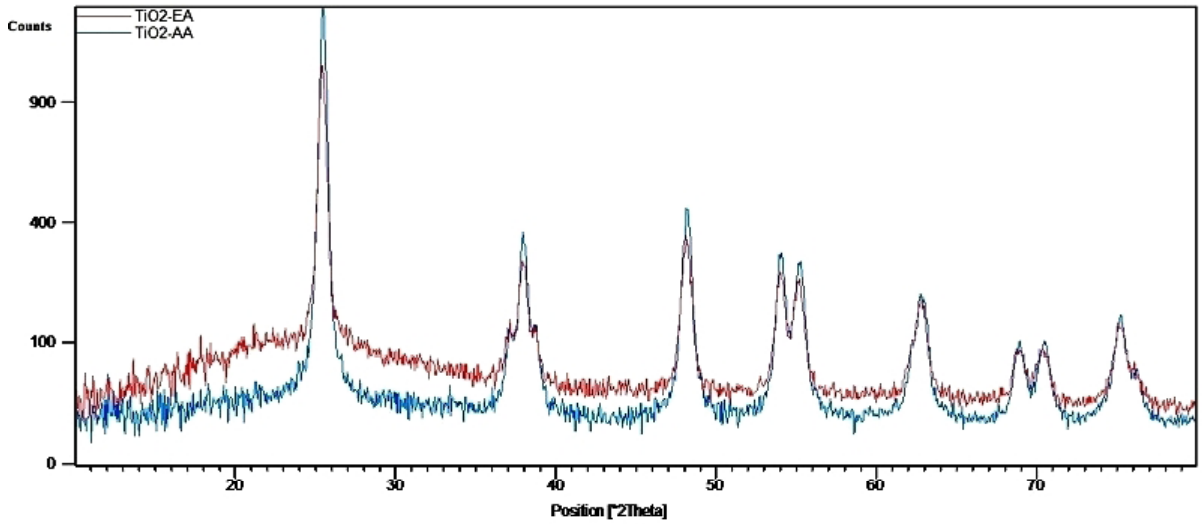

Fig.3. The XRD pattern of TiO_2-AA-450 and TiO_2-EA-450 samples.

samples are 14.1 and 17 nm, respectively. The optimum particle size corresponding to the highest photoactivity in titanium dioxide nanoparticles systems is 10–14 nm [30]. The lattice parameters were determined using these equations: $d_{(hkl)} = \lambda/2\sin\theta$, $1/d_{(hkl)} = (h^2+k^2)/a^2 + l2/c^2$, where $d_{(hkl)}$ is the distance between crystal planes of (hkl), λ is the X-ray wavelength, θ is the diffraction angle of

crystal plane (hkl), hkl is the crystal plane index, and a, b, and c are lattice parameters (in anatase phase of TiO_2, a = b –c) [5]. The parameters of the lattice for the synthesized nanoparticles have been calculated and represented in Table 1. The lattice parameters of the synthesized samples were compared to the anatase phase (a=3.785A° ,C=9.514A°) [31]. Some changes are seen that show the different procedures forming crystalline structures in the samples. Also, a difference in the forming procedure of the crystalline structure was observed in the analysis of the TGA thermogram.

Table 1. The crystallite sizes and lattice parameters of TiO_2-AA and TiO_2-EA nanoparticles

Nano particle	FWHM	Particle size (nm)	Lattice parameters (A^0)	
			a(101)	C(101)
TiO_2-AA	0.5698	14.1	3.766	9.359
TiO_2-EA	0.5011	17	3.739	9.064

It is a well-accepted idea that the diffraction peak's intensity points out the crystallization degree of samples [5] . As shown in Fig. 3, the greater the intensity of the TiO_2-AA peaks suggests the formation of higher crystallinity [32, 33]. High crystallinity, which is a result of a reduction in crystal defects in the structure, can facilitate the separation of photo-generated holes and electrons and leads to a decrease in the recombination chance of charge carriers as well, and so the photocatalytic activity will be increased [34, 35].

Preparing a sample of titanium dioxide nanoparticles in the presence of acetic acid, TiO_2-AA, permits the process of gel formation to be well-controlled. The presence of additional acetate anion at the surface of TiO_2 particles can prevent the growth of TiO_2 nanoparticles. The existance of this kind of complex of acetate anion at the surface of TiO_2 is likely the reason for the decrease in the particle size of TiO_2 synthesized in the sol-gel method using acetic acid as solvent [36, 37]. The additional acetic acid is not due to the impurities on the surface of TiO_2 after calcinations, which is further confirmed by FTIR spectroscopy.

SEM studies were performed to investigate the surface morphology of the synthesized TiO_2-AA and TiO_2-EA nanoparticles. Fig. 4 shows SEM images of the samples calcinated at 450 °C. According to Fig. 4, the grains of the particles are spherical, and the TiO_2-AA nanoparticles were more uniformed than TiO_2-EA. The SEM images show that the agglomeration degree for the TiO_2-EA sample is more than the TiO_2-AA sample and the nanoparticles of TiO_2-AA have a more uniform morphology and smaller particle size. Further observation indicates that the morphology of the TiO_2-AA nanoparticles is very rugged and may be beneficial to enhancing the adsorption of reactants due to its high surface area.

To study the role of the precursor solvent on the TiO_2 surface, the FTIR spectra of TiO_2-AA and TiO_2-EA particles were compared after calcination at 450 °C. As demonstrated in Fig. 5, a broad band at 3400 cm^{-1} area can be observed for both samples which indicates asymmetric and symmetric stretching vibrations of the terminating hydroxyl group (–OH) in the surface of synthesized nanoparticles. In addition, the characteristic peak in 1624 cm^{-1} is related to the O-H bending vibration of the hydroxyl group in the molecule of the adsorbed water which is observed in both samples [18, 38]. These bands are evidence of chemically and physically adsorbed H_2O on the surface of synthesized nanoparticles [39].

The characteristic vibrations of the inorganic Ti-O stretch have been observed in the area below 1000 cm^{-1} [12]. In the low energy area of the spectrum the bands at 461 cm^{-1} are assigned to O-Ti-O and Ti-O-Ti bending vibration, and the broad band at 528 cm^{-1} directs to the vibration of the metal–oxygen bond (Ti–O) in the sample of TiO_2 [10, 39, 40]. As shown in Fig. 5a, the IR band related to Ti-O at 528 cm^{-1} in the TiO_2-AA sample move toward a shorter wavelength and transmit to 586 cm^{-1}. This result shows that the degree of crystallization in the TiO_2-AA sample has been increased which is confirmed by the results of the XRD [40]. It declares that the combination between ethanol and Ti precursor become weak, but the combination between acetic acid and Ti precursor become strong, which is in accordance with the

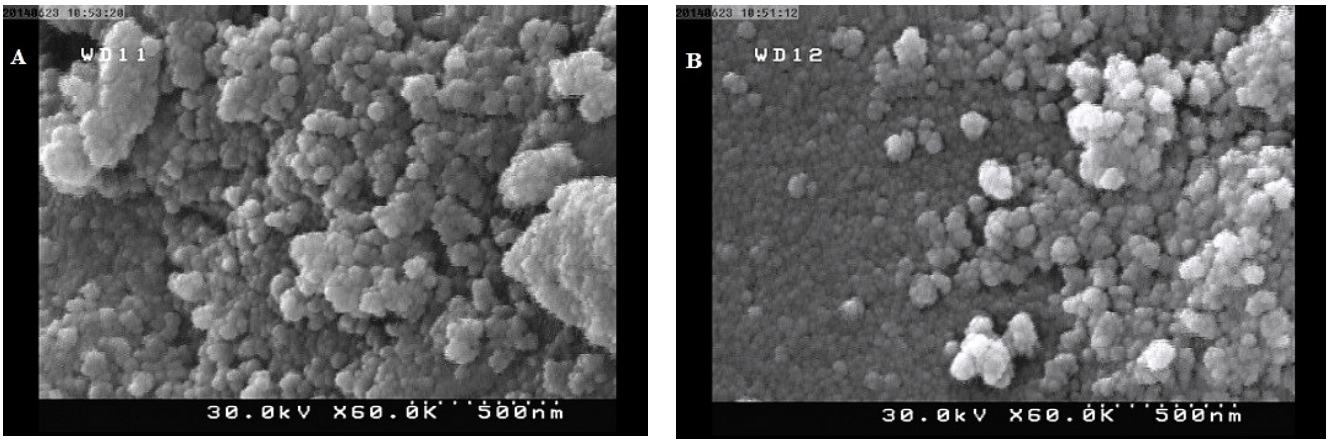

Fig. 4. SEM image of a) TiO_2-AA, b) TiO_2-EA nanoparticles

TGA results. Therefore, elimination of acetic acid is harder than ethanol and affected the crystallinity of the sample.

FTIR spectrum of adsorbed CO_2 on TiO_2 shows four bands: 1586, 1430, 1317, and 1227 cm^{-1}. CO_2 as a Lewis acid can be linked to basic sites with a alkalinity feature in the metal oxides surface. In titanium dioxide with an anatase phase, adsorbed CO_2 produces mainly bidentate carbonate. The surface bidentate carbonate complexes are formed involving the interaction with Ti^{4+}- O^{2-} Lewis acid–base pairs sites in the surface of the anatase phase [41]. These results of the FTIR spectrum suggest that the amount of Ti^{4+}-O^{2-} pairs on the surface of TiO_2-AA is more than that on TiO_2-EA. The spectrum of TiO_2-EA show an OH peak broader than TiO_2-AA, while in the spectrum of TiO_2-AA evidence of adsorb CO_2 is assigned. Adsorption of CO_2 on the surface of TiO_2 nanoparticles leads to a reduction in surface O-H groups so that the reduction of OH peak intensity in 3400 cm^{-1} is identified [42]. As revealed in both spectrums, the organic ligand and the solvent of precursor were completely eliminated after the annealing process. These results match the TGA results which illustrate that at temperatures above 430°C, the mass loss is not observed.

For semiconductor materials, diffuse reflectance spectroscopy (DRS) is an efficient method for characterizing the optical absorption property, which is recognized as one of the important factors for photocatalytic activities [34]. Fig. 6 shows the UV–visible DRS of TiO_2-AA and TiO_2-EA photocatalysts calcined at 450 °C for 2 h. Compared with TiO_2-EA, the absorption edge of TiO_2-AA was shifted towards thelower energy region (i.e. red shift), and the absorption edge was 403 nm. The absorption edge of TiO_2-EA was about 395 nm. Accordingly, the absorption edges of the modified TiO_2 photocatalysts had been shifted into the high wavelength region, causing narrowing of the band gaps [43]. The minimum energy that is required to transfer an electron from the valance band to conductance band depends upon the band-gap energy Ebg of the photocatalyst and is given as $E_{bg}(eV) = 1240/\lambda(nm)$, where λ is the wavelength of the absorption edge in the spectrum [44]. The band gaps for TiO_2-AA and TiO_2-EA were estimated 3.06 and 3.14 eV, respectively. The enhanced absorption light activity was attributed to the good anatase crystallinity and small crystallite size [45].

3.2.Photocatalytic activity

The photocatalytic H_2 evolution from water was investigated over TiO_2-AA and TiO_2-EA samples under natural solar light. The irradiation time dependence on the hydrogen production on TiO_2-AA and TiO_2-EA samples are shown in Figs. 7 and 8, respectively. All samples prepared by sol-gel and modified sol-gel (acetic acid as solvent) showed the photocatalytic activity for hydrogen production from water. The photocatalytic activity of the H_2

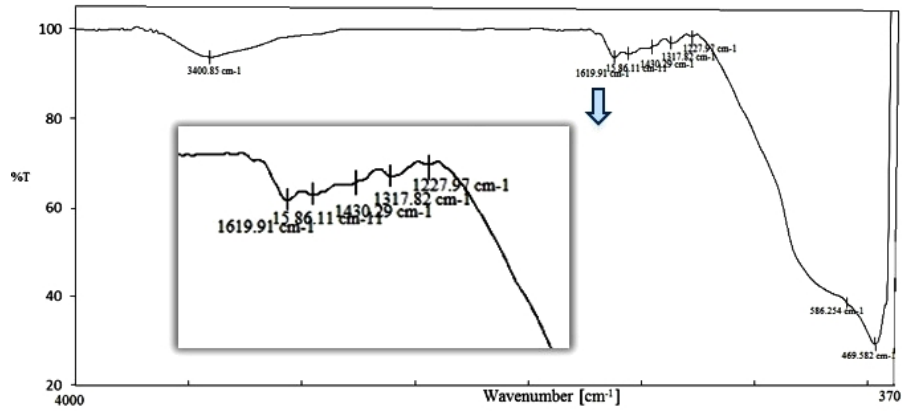

(a)

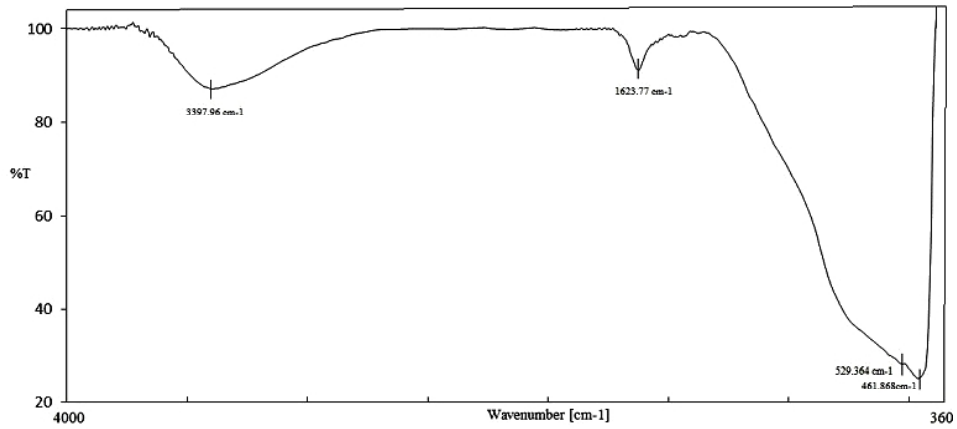

(b)

Fig. 5. FT-IR spectrum of TiO_2 nanoparticles annealed at 450°C a) TiO_2-AA, b) TiO_2-EA.

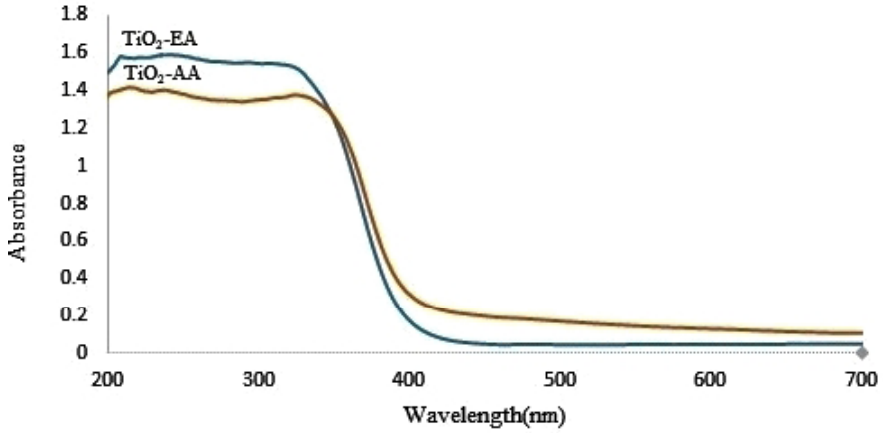

Fig. 6.UV-Vis-DRS of TiO_2-AA and TiO_2-EA nanoparticles

production system can be explained by using the TiO_2 photocatalysis mechanism. Under irradiation with energy greater than the band-gap energy of TiO_2, the formation of electrons (e-) and holes (h+) in the conduction band and valence band occurred which then can migrate toward the TiO_2 surface. The resulting hole has strong oxidizing property and the electron is reduced as well. By reducing the absorbed proton in the photocatalyst surface, the electron can produce H_2 which after entering the water phase can be moved to the gas phase. Simultaneously, the hole can be wiped out by the reaction of hole

scavengers such as methanol and ethanol. Hole scavengers prevent the hole's reaction with water and consequently prevents oxygen production, and as a result the possibility of the backward reaction of hydrogen and oxygen and water production is lessened. Likewise, in the effect of the reaction between hole scavengers and hole, the recombination rate of hole and electron is reduced [46, 47].

Methanol as a hole scavenger can react with the holes and oxidized to aldehyde acid and finally H_2 and CO_2 gases are obtained [3]. In order to prove the effect of methanol as a hole scavenger on hydrogen evolution, the hydrogen evolution on the TiO_2-AA photocatalyst in water without methanol was measured. A trace hydrogen gas, less than the detection limit of our instrument, was seen after 3 h of light irradiation.

It can be seen that the amount of the evolved H_2 is increased with the irradiation time for TiO_2-AA and TiO_2-EA samples as shown in Figs. 7 and 8, respectively. The consequent fall in activity from 450ºC to 650ºC is due to the combined action of various factors: the lower surface area and the growth of nanoparticle size [22]. The highest activity was observed for TiO_2-AA-450 with an average hydrogen production rate of 770 (umol/h.g).

The H_2 production activity of the Degussa P25 was compared with TiO_2-AA and TiO_2-EA samples (shown in Figs. 7 and 8). The Degussa P25 powder, which is a mixture of the anatase and rutile phases (70–85% anatase, 30–15% rutile), has been used as a standard TiO_2 reference material [48]. Potential of the conduction band of the anatase phase is at a more

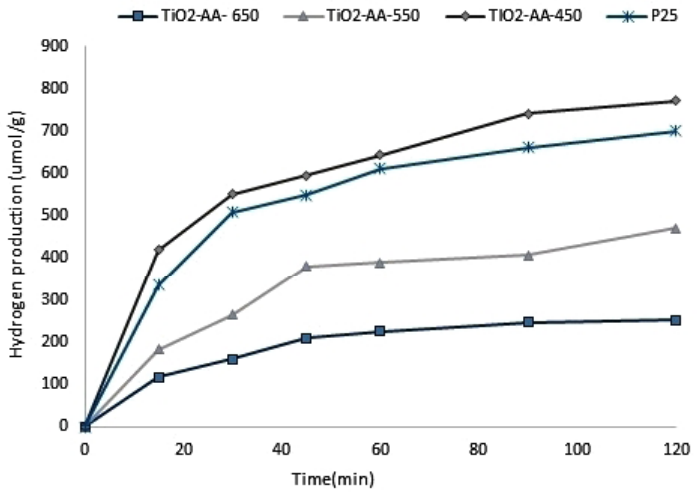

Fig.7. The rate of hydrogen evaluation using TiO_2-AA and P25 samples

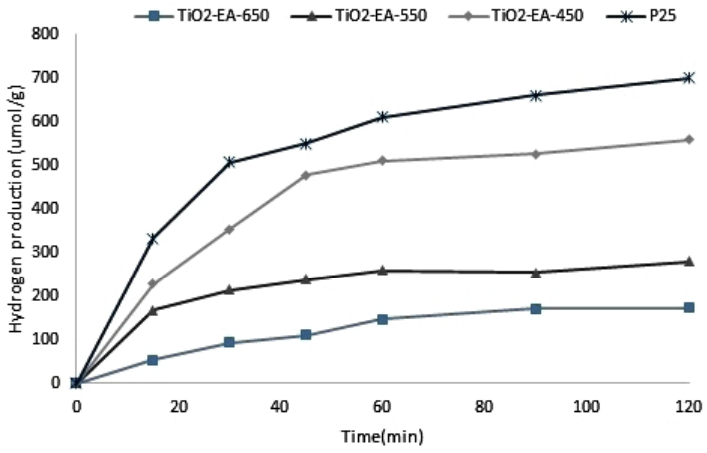

Fig. 8. The rate of hydrogen evaluation using TiO_2-EA and P25 samples

negative position than that of the rutile phase. Thus, the excited electrons easily transfer H^+ ions on the surface of TiO_2 having an anatase phase [49]. The H_2 formation process should be more efficient on the anatse-TiO_2(101) surface analogous to the rutile-TiO_2(110) surface [50].

In order to study the effect of the precursor solvent on the photocatalytic activity of the TiO_2 nanoparticles, hydrogen production rate of the nanoparticles was compared. All synthesized samples have an anatase phase; however, there is a difference in the photocatalytic activity of the particles with the same phase which indicates that in addition to the crystal phase, other factors impact nanoparticles activity [20]. It is believed that the process of producing nano photocatalyst has an important role in the higher activity of produced photocatalyst [51]. We demonstrated that in the present study, the sol-gel method using acetic acid as a solvent of Ti precursor is a better way to synthesize TiO_2 than the sol gel (ethanol) method.

It is obvious that catalytic activity of a solid catalyst largely depends on the catalyst surface [41]. While TiO_2 surfaces do not create a strong link with molecular hydrogen, various types of adsorption of hydrogen atoms in the surface of TiO_2 have been reported e.g. bridging hydroxyls, hydride-type H-Ti species and subsurface hydroxyls [52, 53].

After laboratory examinations, Xu et al. presented that molecular hydrogen can be produced in the effect of thermal recombination reaction of hydrogen atoms on bridge hydroxyls. Studies show that bridging hydroxyl species do not have photoactive properties but hydride-type H-Ti species have been known as the photoactive surface particles [52, 54].

CO_2 adsorption on the anatase phase surface indicates that $Ti^{4+}O^{2-}$ density on the surface of TiO_2-AA is more than the TiO_2-EA sample. This is an indicative of a greater percentage of H-Ti on TiO_2-AA surface, which accordingly confirms more photoactive hydrogen molecule production in the TiO_2-AA sample compared to the TiO_2-EA sample [41]. These results illustrate that the precursor solvent had an effect on the photocatalyst surface and as a result has an effect on the photocatalytic activity. Furthermore, since a high quality of crystallinity in photocatalytic hydrogen production in water splitting process is preferred over a high surface area, in the conducted examinations TiO_2-AA samples with a higher quality of crystallinity presented higher hydrogen production [55].

4. Conclusion

In sol-gel processes, the final product morphology is strongly influenced by the reactivity of the precursor. In the present study, we demonstrated that acetic acid is a better solvent for athe precursor of Ti to synthesize TiO_2 nanoparticles versus ethanol. The TiO_2 nanoparticles were synthesized with smaller size and higher crystallinity with a selection of acetic acid solvent. These results showed that the precursor solvent affected the surface of the catalyst and the crystallinity of TiO_2 nanoparticles and resulted in higher activity of the photocatalyst for H_2 production.

Acknowledgment

The authors are grateful to the Council of Maleke Ashtar University of Technology for providing financial support to undertake this work.

References

[1] Vinothkumar N., De M., “Enhanced photocatalytic hydrogen production from water–methanol mixture using cerium and nonmetals (B/C/N/S) co-doped titanium dioxide”. Mater Renew Sustain Energy. 2014, 3:25

[2] Ismail A a., Bahnemann D.W. , “Photochemical splitting of water for hydrogen production by photocatalysis: A review”, Sol Energy Mater Sol Cells , 2014, 128:85.

[3] Hakamizadeh M., Afshar S., Tadjarodi A., et. al., “Improving hydrogen production via water splitting

over Pt/TiO_2/activated carbon nanocomposite". Int. J. Hydrogen Energy 2014, 39:7262.

[4] Hong E., Choi J., Kim J. H. " Monolithic film photocatalyst and its application for hydrogen production with repeated unit structures", Thin Solid Films, 2013, 527:363.

[5] Moradi H., Eshaghi A., Rahman S., Ghani K., " Ultrasonics Sonochemistry Fabrication of Fe-doped TiO_2 nanoparticles and investigation of photocatalytic decolorization of reactive red 198 under visible light irradiation", Ultrason Sonochem, 2016, 32:314.

[6] You X., Chen F., Zhang J., " Effects of calcination on the physical and photocatalytic properties of TiO_2 powders prepared by sol-gel template method". J. Sol-Gel Sci Technol , 2005, 34:181.

[7] Vetrivel V., Rajendran K., Kalaiselvi V., " Synthesis and characterization of Pure Titanium dioxide nanoparticles by Sol- gel method", International Journal of ChemTech Research, 2015, 7:1090.

[8] Aranda M. S., Pineda M., Hernández J., et. al., "Redalyc.Physical properties of TiO_2 prepared by sol-gel under different pH conditions for photocatalysis", Superficies y Vacío, 2005, 18:46.

[9] Sahu M., Biswas P., "Single-step processing of copper-doped titania nanomaterials in a flame aerosol reactor", Nanoscale Res Lett, 2011, 6:441.

[10] Sugapriya S., Sriram R., Lakshmi S., " Effect of annealing on TiO_2 nanoparticles", Optik , 2013, 124:4971.

[11] Wetchakun N., Incessungvorn B., Wetchakun K., Phanichphant S.,"Influence of calcination temperature on anatase to rutile phase transformation in TiO_2 nanoparticles synthesized by the modified sol–gel method". Mater Lett, 2012, 82:195.

[12] Hamadanian M., Reisi-Vanani A., Majedi A., "Synthesis, characterization and effect of calcination temperature on phase transformation and photocatalytic activity of Cu,S-codoped TiO_2 nanoparticles". Appl Surf Sci., 2010, 256:1837.

[13] Wang Y., He Y., Lai Q., Fan M., "Review of the progress in preparing nano TiO_2: An important environmental engineering material", J. Environ Sci., 2014, 26:2139.

[14] Fröschl T., Hörmann U., Kubiak P., et. al., "High surface area crystalline titanium dioxide: potential and limits in electrochemical energy storage and catalysis", Chem. Soc. Rev., 2012, 41:5313.

[15] Xin G., Yu B., Pan H., Wen B., " Enhancement of photocatalysis for H_2 evolution on annealed Nano-Titania". Mater Sci. Semicond Process, 2014, 25:153–158.

[16] Vijayalakshmi R., Rajendran V., "Synthesis and characterization of nano-TiO_2 via different methods", 2012, 4:1183–1190.

[17] Loryuenyong V, Jarunsak N, Chuangchai T, Buasri A., "The photocatalytic reduction of hexavalent chromium by controllable mesoporous anatase TiO_2 nanoparticles". Adv Mater Sci Eng.(2014) 348427.

[18] Luo S, Wang ÆF, Shi ÆZ "Preparation of highly active photocatalyst anatase TiO_2 by mixed template method", 2009, 1–7.

[19] Dinh CT, Nguyen TD, Kleitz F, Do TO "A solvothermal single-step route towards shape-controlled titanium dioxide nanocrystals". Can J. Chem. Eng., 2012, 90:8–17.

[20] Naghibi S, Faghihi Sani MA, Madaah Hosseini HR "Application of the statistical Taguchi method to optimize TiO_2 nanoparticles synthesis by the hydrothermal assisted sol-gel technique". Ceram Int., 2014, 40:4193–4201.

[21] Zhang P, Tang B, Xia W, et al "Preparation and Characterizations of TiO_2 Nanoparticles by Sol-Gel Process using DMAC Solvent".(MMECEB 2015), 2016, 892–895.

[22] Melián E.P., Suárez M.N., Jardiel T, et. al.," Influence of nickel in the hydrogen production activity of TiO_2", Appl Catal B Environ, 2014, 192:152.

[23] Delekar S.D., Yadav H.M., Achary S.N., et. al., "Structural refinement and photocatalytic activity of Fe-doped anatase TiO_2 nanoparticles", Appl Surf Sci, 2012, 263:536.

[24] Sun T., Liu E., Fan J., et. al., "High photocatalytic activity of hydrogen production from water over Fe doped and Ag deposited anatase TiO_2 catalyst synthesized by solvothermal method", Chem. Eng. J., 2013, 228:896.

[25] D'Arienzo M., Dozzi M.V., Redaelli M., et al. "Crystal Surfaces and Fate of Photogenerated Defects in Shape Controlled Anatase Nanocrystals: Drawing Useful Relations to Improve the H_2 yield in Methanol Photosteam Reforming", J. Phys. Chem. C., 2015, 119 (22):12385.

[26] Deng F., Luo X., Li K., et. al., "The effect of vinyl-containing ionic liquid on the photocatalytic activity of iron-doped TiO2", J. Mol. Catal. A Chem., 2013, 366:222.

[27] Barakat NAM., Kanjwal M.A., Chronakis I.S., Kim H.Y. "Influence of temperature on the photodegradation process using Ag-doped TiO_2 nanostructures: Negative impact with the nanofibers", J. Mol. Catal. A Chem., 2013, 366:333.

[28] Suwarnkar MB., Dhabbe RS., Kadam AN., Garadkar KM."Enhanced photocatalytic activity of Ag doped TiO_2 nanoparticles synthesized by a microwave assisted method", Ceram Int., 2014, 40:5489

[29] H. R. Pouretedal, O. shevidi, M. Nasiri, " Red water treatment by photodegradation process in presence of modified TiO_2 nanoparticles and validation of treatment efficiency by MLR technique". J. Iran Chem. Soc., 2016, 3–10.

[30] Mohamed RM., McKinney DL., Sigmund WM., "Enhanced nanocatalysts", Mater Sci. Eng. R. Reports, 2012, 73:1.

[31] Hanaor DAH., Sorrell CC., " Review of the anatase to rutile phase transformation"., 2011, 855–874.

[32] He F., Ma F., Li T., Li G, "Solvothermal synthesis of N-doped TiO_2 nanoparticles using different nitrogen sources and their photocatalytic activity for degradation of benzene", Chinese J. Catal., 2013, 34:2263.

[33] Liu D.R., Wei C.D., Xue B., et. al. "Synthesis and photocatalytic activity of N-doped $NaTaO_3$ compounds calcined at low temperature", J. Hazard Mater, 2010, 182:50.

[34] Wang Q., Lian J., Bai Y., et al., "Materials Science in Semiconductor Processing Photocatalytic activity of hydrogen production from water over TiO_2 with different crystal structures", Mater Sci Semicond Process , 2015, 40:418.

[35] Cheng X., Yu X., Xing Z., Yang L., "Synthesis and characterization of N-doped TiO_2 and its enhanced visible-light photocatalytic activity. Arab J. Chem., 2012, 4:052

[36] Hamadanian M., Reisi-vanani A., Behpour M., Esmaeily AS., "Synthesis and characterization of Fe, S-codoped TiO_2 nanoparticles :Application in degradation of organic water pollutants", DES , 2011, 281:319.

[37] Campostrini R., Ischia M., Palmisano L., "Pyrolysis study of sol-gel derived TiO_2 powders: part III.TiO_2 anatase prepared by reacting titanium(IV) isopropoxide with acetic acid", Journal of Thermal Analysis and Calorimetry. 2004, 75:13

[38] Hanaor D. H., Chironi I., Karatchevtseva I., et. al. "Single and mixed phase TiO_2 powders prepared by excess hydrolysis of titanium alkoxide", Adv Appl Ceram, 2012, 111:149.

[39] Praveen P., Viruthagiri G., Mugundan S., Shanmugam N., "Sol-gel synthesis and characterization of pure and manganese doped TiO2 nanoparticles--a new NLO active material", Spectrochim Acta A Mol Biomol Spectrosc, 2014, 120:548

[40] Cheng X., Yu X., Xing Z., "Characterization and mechanism analysis of N doped TiO_2 with visible light response and its enhanced visible activity", Appl. Surf. Sci., 2012, 258:3244.

[41] Su W., Zhang J., Feng Z., et. al. "Surface Phases of TiO_2 Nanoparticles Studied by UV Raman Spectroscopy and FT-IR Spectroscopy", J. Phys. Chem., 2008, 112:7710.

[42] Kaur M., Verma NK., "$CaCO_3$ /TiO_2 Nanoparticles Based Dye Sensitized Solar Cell", J. Mater. Sci. Technol., 2014, 30:328.

[43] Chen H., Jin H., Dong B., "Preparation of magnetically supported chromium and sulfur co-doped TiO_2 and use for photocatalysis under visible light", Research on Chemical Intermediates, 2012, 38: 2335.

[44] H. R. Pouretedal, A. M. Sohrabi. "Photosensitization of TiO_2 by ZnS and bromo thymol blue and its application in photodegradation of para-nitrophenol". J. Iran Chem. Soc., 2016, 13:73–79.

[45] Cheng X., Yu X., Xing Z."Enhanced photoelectric property and visible activity of nitrogen doped TiO_2 synthesized from different nitrogen dopants", Appl Surf Sci., 2013, 268:204.

[46] Puangpetch T., Chavadej S., Sreethawong T. "Hydrogen production over Au-loaded mesoporous-assembled $SrTiO_3$ nanocrystal photocatalyst: Effects of molecular structure and chemical properties of hole scavengers", Energy Convers Manag, 2011, 52:2256.

[47] Khan MA., Woo SI., Yang OB., "Hydrothermally stabilized Fe(III) doped titania active under visible light for water splitting reaction", Int. J. Hydrogen Energy, 2008, 33:5345.

[48] Yuan J., Chen M, Shi J., Shangguan W., "Preparations and photocatalytic hydrogen evolution of N-doped TiO_2 from urea and titanium tetrachloride", Int. J. Hydrogen Energy, 2006, 31:1326.

[49] Nishijima K., Kamai T., Murakami N, et. al., "Photocatalytic Hydrogen or Oxygen Evolution from Water over S- or N-Doped TiO_2 under Visible Light", Int. J. Photoenergy, 2007, 2008:1.

[50] Xu C., Yang W., Guo Q., et. al., "Molecular Hydrogen Formation from Photocatalysis of Methanol on Anatase-TiO_2 (101)", J. Am. Chem. Soc., 2014, 136:602.

[51] Kimi M., Yuliati L., Shamsuddin M. "Photocatalytic hydrogen production under visible light over $Cd_{0.1}Sn_xZn_{0.9-2x}S$ solid solution photocatalysts", Int. J. Hydrogen Energy, 2011, 36:9453.

[52] Wu Z., Zhang W., Xiong F., et al., "Active hydrogen species on TiO_2 for photocatalytic H_2 production",Phys. Chem. Chem. Phys., 2014, 16:7051.

[53] Qing G., Chuanyao Z., Zhibo M.,et. al., "Elementary photocatalytic chemistry on TiO_2 surfaces", Chem. Soc. Rev., 2016, 45:3701.

[54] Xu C., Yang W., Guo Q., et al. "Molecular Hydrogen Formation from Photocatalysis of Methanol on TiO_2(110) BT", Journal of the American Chemical Society, 2013, 2:1–4.

[55] Zuo F., Wang L., Feng P., "Self-doped Ti^{3+}@ TiO_2 visible light photocatalyst: Influence of synthetic parameters on the H_2 production activity", Int. J. Hydrogen Energy, 2014, 39:711.